ACCEPTED FOR PUBLICATION IN APJ; UTAP-417
Preprint typeset using LaTeX style emulateapj v. 25/04/01

arXiv:astro-ph/0207520v1 24 Jul 2002

CONSTRAINTS ON THE BARYONIC COMPRESSION AND IMPLICATIONS FOR THE FRACTION OF DARK HALO LENSES

MASAMUNE OGURI
Department of Physics, School of Science, University of Tokyo, Tokyo 113-0033, Japan.
oguri@utap.phys.s.u-tokyo.ac.jp
Accepted for publication in ApJ; UTAP-417

ABSTRACT

We predict the fraction of dark halo lenses, that is, the fraction of lens systems produced by the gravitational potential of dark halos, on the basis of a simple parametric model of baryonic compression. The fraction of dark halo lenses primarily contains information on the effect of baryonic compression and the density profile of dark halos, and is expected to be insensitive to cosmological parameters and source population. The model we adopt comprises the galaxy formation probability $p_{\rm g}(M)$ which describes the global efficiency of baryonic compression and the ratio of circular velocities of galaxies to virial velocities of dark halos $\gamma_{\nu} = v_{\rm c}/v_{\rm vir}$ which means how the inner structure of dark halos is modified due to baryonic compression. The model parameters are constrained from the velocity function of galaxies and the distribution of image separations in gravitational lensing, although the degeneracy between model parameters still remains. We show that the fraction of dark halo lenses depends strongly on γ_{ν} and the density profile of dark halos such as inner slope α. This means that the observation of the fraction of dark halos can break the degeneracy between model parameters if the density profile of dark halo lenses is fully settled. On the other hand, by restricting γ_{ν} to physically plausible range we can predict the lower limit of the fraction of dark halo lenses on the basis of our model. Our result indicates that steeper inner cusps of dark halos ($\alpha \gtrsim 1.5$) or too centrally concentrated dark halos are inconsistent with the lack of dark halo lenses in observations.

Subject headings: cosmology: theory — dark matter — galaxies: formation — galaxies: halos — galaxies: clusters: general — gravitational lensing

1. INTRODUCTION

Strong gravitational lensing offers a powerful probe of the matter distribution in the universe. So far ~ 60 lensed quasars are known, and their properties are summarized by CfA/Arizona Space Telescope Lens Survey (CASTLES[1]). Most of these lens systems have image separations $\theta \lesssim 3''$. The cold dark matter (CDM) scenario, however, predicts sufficiently cuspy dark halos (e.g., Navarro, Frenk, & White 1996, 1997), thus dark halos can produce the significant amount of multiple images even at $\theta \gtrsim 3''$ (Wyithe, Turner, & Spergel 2001; Keeton & Madau 2001; Takahashi & Chiba 2001; Li & Ostriker 2002; Oguri et al. 2002). It has been unclear whether the distribution of image separations should be computed based on galaxies (using the luminosity function and the density profile of galaxies; Turner, Ostriker, & Gott 1984; Turner 1990; Fukugita & Turner 1991; Fukugita et al. 1992; Maoz & Rix 1993; Kochanek 1996; Chiba & Yoshii 1999) or dark halos (using the mass function and the density profile of dark halos; Narayan & White 1988; Cen et al. 1994; Wambsganss et al. 1995; Kochanek 1995; Maoz et al. 1997; Wambsganss, Cen, & Ostriker 1998; Mortlock & Webster 2000; Wyithe, Turner, & Spergel 2001; Keeton & Madau 2001; Takahashi & Chiba 2001; Oguri et al. 2002). The distribution of image separations, however, clearly indicates that the use of only dark matter properties cannot match observations. That is, the observed distribution of image separations is never reproduced from the theoretical calculation using the mass function of dark halos and only one population for lensing objects (e.g., Li & Ostriker 2002). The possible solution to explain the distribution of image separations is the modification of inner structure of dark halos by introducing baryonic cooling (Keeton 1998; Porciani & Madau 2000; Kochanek & White 2001; Keeton 2001; Sarbu, Rusin, & Ma 2001; Li & Ostriker 2002). In this picture, inside low mass halos baryons are efficiently compressed and form sufficiently concentrated galaxies, while inside larger halos such as group- or cluster-mass halos global baryon cooling hardly occurs and thus the inner structure of dark halos remains unmodified.

Then a question comes to our mind: *what is the fraction of dark halo lenses?* Here the term "dark halo lenses" is used to describe lenses which are produced by the gravitational potential of dark halos. In other words, the lens objects of dark halo lenses are dark halos which have no central galaxies or have central galaxies but they are too small to dominate in gravitational lensing. Dark halo lenses exhibit characteristic properties such as the small flux ratios and the detectable odd images (Rusin 2002), thus can be distinguished from usual galaxy lenses. Since dark halos are expected to have a steep central cusp, the significant amount of dark halo lenses should be observed. But so far no confirmed dark halo lens system is observed in strong gravitational lensing survey. The exception is arc statistics in rich clusters (Bartelmann et al. 1998; Williams, Navarro, & Bartelmann 1999; Meneghetti et al. 2001; Molikawa & Hattori 2001; Oguri, Taruya, & Suto 2001; Oguri 2002), but the known cluster lenses were all found by searching for lenses in detail after identifying a rich cluster. In the surveys which first identify source objects and see whether they are lensed or not, it seems that dark halo lenses have not been observed yet: statistical argument (Kochanek, Falco, & Muñoz 1999) and individual properties (Rusin 2002) imply that current ambiguous quasar pairs are likely to be binary quasars. Even known lensing systems in clusters, such as Q0957+561 (Walsh, Carswell, & Weymann 1979), are produced mainly by a galaxy in the cluster. The cluster potential contributes to lensing only

[1] Kochanek, C. S., Falco, E. E., Impey, C., Lehar, J., McLeod, B., & Rix, H.-W., http://cfa-www.harvard.edu/castles/

as a perturbation. Therefore, it should be checked whether the lack of dark halo lenses in observations really reconciles with the theoretical prediction.

Description of baryonic effects needs detailed models for the star formation and feedback (e.g., Cole et al. 2000). Instead, in this paper we predict the expected fraction of dark halo lenses on the basis of a simple (minimal) parametric model (Kochanek 2001). This model comprises the formation probability of galaxies, $p_{\rm g}(M)$, and the ratio of circular velocities of galaxies to virial velocities of dark halos, $\gamma_{\rm v}$. The former describes the global efficiency of baryonic compression, and the latter models the modification of inner structure of dark halos due to baryonic compression. The model parameters are chosen so as to reproduce the velocity function of galaxies and the distribution of image separations. Although there remains the strong degeneracy between model parameters, this degeneracy can be broken from the observation of the fraction of dark halos if we fix the density profile of dark halos. On the other hand, by restricting a range of $\gamma_{\rm v}$ from various theories and observations, we can also derive the lower limit of the fraction of dark halo lenses. Our main finding is that steep inner slopes of dark halos ($\alpha \gtrsim 1.5$) or too centrally concentrated dark halos are inconsistent with the lack of dark halo lenses in observations, even if various uncertainties are taken into account. Although this constraint on the density profile is not so severe, a large lens sample obtained by e.g., Sloan Digital Sky Survey (SDSS) can put tighter constraints on the density profile of dark halos as well as the model of baryonic compression.

The plan of this paper is as follows. In §2, we describe the model of baryonic compression. Section 3 is devoted to constrain the model parameters, and §4 presents our predictions for the fraction of dark halo lenses. Finally, we summarize conclusions in §5. Throughout this paper, we assume the lambda-dominated cosmology $(\Omega_0, \lambda_0, h, \sigma_8) = (0.3, 0.7, 0.7, 1.04)$, where the Hubble constant in units of $100{\rm km\,s^{-1}Mpc^{-1}}$ is denoted by h. As shown below, however, our results are quite insensitive to a particular choice of cosmological parameters.

2. THEORETICAL MODEL

2.1. *Effects of Baryons on Dark Halos*

The obvious difference between velocity functions of galaxies and dark halos at high velocity (e.g., Gonzalez et al. 2000) indicates that the efficiency of the baryon compression changes from galaxy-mass scale to group- and cluster-mass scales. If the mass of dark halos is sufficiently large, the baryon cooling time $\tau_{\rm cool}$ which increases with halo mass (e.g., Cole et al. 2000) becomes larger than the age of dark halos which slightly deceases with halo mass (e.g., Lacey & Cole 1993; Kitayama & Suto 1996). Thus baryons inside such a massive dark halo do not form so large galaxies as to collect most of baryons in the dark halo. This yields a steep cutoff at high velocity in the galaxy velocity function. To model this, following Kochanek (2001), we introduce the probability $p_{\rm g}(M)$ that a sufficiently large galaxy which collects most of internal baryons is formed inside a halo of mass M. For example, galaxy-mass halos with mass M usually have large galaxies with mass $M_{\rm gal} \sim (\Omega_{\rm b}/\Omega_0)M$. On the other hand, groups or clusters also have galaxies but their mass are small even for galaxies which lie at the center of halos, $M_{\rm gal} \ll (\Omega_{\rm b}/\Omega_0)M$, here in this case $M \gtrsim 10^{13}h^{-1}M_\odot$ (e.g., Yoshikawa et al. 2001). Therefore we regard galaxies in groups or clusters as "substructures" and do not take into account. We adopt a parametric model (Kochanek 2001)

$$p_{\rm g}(M) = \begin{cases} 1 & (M < M_{\rm h}), \\ \exp\left[1 - \left(\dfrac{M}{M_{\rm h}}\right)^{\delta_{\rm h}}\right] & (M > M_{\rm h}). \end{cases} \tag{1}$$

Although the overall factor of $p_{\rm g}(M)$ should become another parameter, we neglect it. The effect of the overall factor of $p_{\rm g}(M)$ on the fraction of dark halo lenses will be discussed in §4.

Also, there is a difference in the slopes of velocity functions of dark halos and galaxies at small velocity (e.g., Gonzalez et al. 2000; Nagamine et al. 2001), and this demands the modification of $p_{\rm g}(M)$ at low M. We, however, neglect this effect because we are not interested in low velocity galaxies which hardly contribute to lensing statistics.

The baryon compression also changes inner structure of dark halos (e.g., Blumenthal et al. 1986; Mo, Mao, & White 1998). Before the baryon cooling occurs, we assume that the density profile of dark halos is well described by the one-parameter family of the form (Zhao 1996; Jing & Suto 2000)

$$\rho(r) = \frac{\rho_{\rm crit}\delta_{\rm c}}{\left(r/r_{\rm s}\right)^{\alpha}\left(1+r/r_{\rm s}\right)^{3-\alpha}}, \tag{2}$$

where $r_{\rm s} = r_{\rm vir}/c_{\rm vir}$ and $c_{\rm vir}$ is the concentration parameter. We adopt the mass and redshift dependence reported by Bullock et al. (2001):

$$c_{\rm vir}(M,z) = \frac{8}{1+z}\left(\frac{M}{10^{14}h^{-1}M_\odot}\right)^{-0.13}, \tag{3}$$

for $\alpha = 1$, and generalize it to $\alpha \neq 1$ by multiplying the factor $(2-\alpha)$ (Keeton & Madau 2001). We also take account of scatter of the concentration parameter which has a log-normal distribution with the dispersion of $\sigma_{\rm c} = 0.18$ (Jing 2000; Bullock et al. 2001). The characteristic density $\delta_{\rm c}$ can be computed using the spherical collapse model (see Oguri et al. 2001). While the correct value of α is still unclear, the existence of a cups with $1 \lesssim \alpha \lesssim 1.5$ has been established in recent N-body simulations (Navarro et al. 1996, 1997; Moore et al. 1999; Ghigna et al. 2000; Jing & Suto 2000; Klypin et al. 2001; Fukushige & Makino 2001, 2002; Power et al. 2002).

Next consider the modification of inner structure of dark halos induced by baryonic compression. In general, cooled baryons (galaxies) are more centrally concentrated than dark matters. Although complicated physical models are needed to know the modified mass distribution, we simply assume that the mass distribution of galaxies is well described by the Singular Isothermal Sphere (SIS) approximation:

$$\rho(r) = \frac{\sigma^2}{2\pi G r^2}, \tag{4}$$

where σ is a one-dimensional velocity dispersion and is related to the circular velocity $v_{\rm c}$ as $v_{\rm c} = \sqrt{2}\sigma$. We also assume that $v_{\rm c}$ as a function of halo mass M can be described as

$$\gamma_{\rm v} = \frac{v_{\rm c}}{v_{\rm vir}(M)}, \tag{5}$$

where $v_{\rm vir}(M)$ is the halo virial velocity defined by $v_{\rm vir}(M) = \sqrt{GM/r_{\rm vir}}$ and $\gamma_{\rm v}$ is an arbitrary constant. The SIS approximation for galaxies is consistent with several observations such as dynamics (e.g., Rix et al. 1997) and gravitational lensing (e.g., Rusin & Ma 2001; Cohn et al. 2001).

2.2. *Velocity Function of Galaxies*

Once the probability $p_g(M)$ and the galaxy circular velocity $v_c(M)$ are given, we can calculate the velocity function of galaxies from the mass function of dark halos:

$$\frac{dn}{dv_c}(v_c(M)) = p_g(M)\left|\frac{dv_c(M)}{dM}\right|^{-1}\frac{dn}{dM}(M). \quad (6)$$

For the mass function dn/dM, we adopt a fitting form derived by Sheth & Tormen (1999):

$$\frac{dn_{ST}}{dM} = 0.322\left[1+\left(\frac{\sigma_M^2}{0.707\delta_0^2(z)}\right)^{0.3}\right]\sqrt{\frac{1.414}{\pi}} \times\frac{\rho_0}{M}\frac{\delta_0(z)}{\sigma_M^2}\left|\frac{d\sigma_M}{dM}\right|\exp\left[-\frac{0.707\delta_0^2(z)}{2\sigma_M^2}\right]. \quad (7)$$

This fitting form coincides more accurately with numerical simulations than the analytic mass function derived by Press & Schechter (1974). The velocity function is sometimes expressed in terms of $\log v_c$ as

$$\Psi(v_c) = \frac{dn}{d\log v_c}. \quad (8)$$

In this calculation we neglect the contribution from "substructures" (i.e., galaxies in groups and clusters), because this mainly changes the normalization of the velocity function which we do not use as a constraint on the model parameters (see §3.1). Substructures, however, may affect the fraction of dark halo lenses directly, because it changes only the number of galaxy lenses. Therefore we consider the effect of substructures in predicting the fraction of dark halo lenses (see §4).

2.3. *Lensing Probability Distribution*

Bearing the picture described in §2.1 in mind, we calculate the probability of gravitational lensing caused by bright galaxies and dark halos separately:

$$P_{gal}(>\theta; z_S, L) = \int_0^{z_S} dz_L \int_{M_{min}}^{\infty} dM\, p_g(M)\sigma_{SIS} B\frac{c\,dt}{dz_L}(1+z_L)^3\frac{dn}{dM}, \quad (9)$$

$$P_{dark}(>\theta; z_S, L) = \int_0^{z_S} dz_L \int_{M_{min}}^{\infty} dM\,\{1-p_g(M)\}\,\sigma_{NFW} B\frac{c\,dt}{dz_L}(1+z_L)^3\frac{dn}{dM}, \quad (10)$$

where z_S is the source redshift, z_L is the lens redshift, L is the luminosity of the source, and dn/dM is the comoving number density of dark halos (eq. [7]). Lensing cross sections σ_{SIS} and σ_{NFW} are given by

$$\sigma_{SIS} = 16\pi^3\left(\frac{\sigma}{c}\right)^4\left(\frac{D_{OL}D_{LS}}{D_{OS}}\right)^2, \quad (11)$$

$$\sigma_{NFW} = \pi\left(\eta_{rad}\frac{D_{OL}}{D_{OS}}\right)^2, \quad (12)$$

where η_{rad} is the radius of the radial caustic at source plane (e.g., Schneider, Ehlers, & Falco 1992) and D_{OL}, D_{OS}, and D_{LS} are the angular diameter distances to the lens, to the source, and between the lens and source, respectively. The one-dimensional velocity dispersion σ in equation (11) can be represented as a function of halo mass M:

$$\sigma = \frac{v_c}{\sqrt{2}} = \frac{\gamma_v v_{vir}(M)}{\sqrt{2}}, \quad (13)$$

where equation (5) is used. The lower limit of integral by mass, M_{min}, is determined by solving the equation $\theta = \theta(M_{min}, z_S, z_L)$. The magnification bias (Turner 1980; Turner et al. 1984) is included in B as follows:

$$B = \frac{1}{\sigma_{lens}\Phi(z_S, L)}\int_{multi} d^2\eta\,\Phi(z_S, L/\mu(\vec{\eta}))\frac{1}{\mu(\vec{\eta})}, \quad (14)$$

where $\Phi(z_S, L)$ is the luminosity function of sources and $\mu(\vec{\eta})$ is the magnification factor at $\vec{\eta}$.

The total lensing probability with image separation larger than θ is given by

$$P(>\theta; z_S, L) = P_{gal}(>\theta; z_S, L) + P_{dark}(>\theta; z_S, L). \quad (15)$$

3. CONSTRAINTS ON THE MODEL

3.1. *Velocity Function of Galaxies*

The velocity function is valuable because it is easy to handle theoretically, and is useful to test the model of galaxy formation and cosmology (Cole & Kaiser 1989; Shimasaku 1993; Gonzalez et al. 2000; Kochanek & White 2001). Using the model described in §2.2, we can calculate the velocity function of galaxies from the mass function of dark halos. By comparing the theoretical velocity function with observed velocity functions, one can constrain the model parameters such as δ_h, M_h, and γ_v. The definite theoretical prediction, however, needs the *correct* value of cosmological parameters such as σ_8. Therefore we use the normalized velocity function

$$\psi(v_c) \equiv \frac{\Psi(v_c)}{\Psi(200\mathrm{km/s})}, \quad (16)$$

instead of $\Psi(v_c)$. Moreover, by using $\psi(v_c)$ we can neglect the effect of the overall factor of $p_g(M)$. For the observed velocity functions, we use five velocity functions derived by Gonzalez et al. (2000): velocity functions derived from Southern Sky Redshift Survey (SSRS2), Automatic Plate Measuring facility survey (APM), United Kingdom Schmidt Telescope survey (UKST), Las Campanas Redshift Survey (LCRS), and K-band survey by Gardner et al. (1997). We restrict the comparison with observations in the region $200\mathrm{km/s} < v_c < 500\mathrm{km/s}$ because of the following two reasons. One reason is that observed velocity functions are not reliable at the high velocity region ($v_c > 500\mathrm{km/s}$) (Gonzalez et al. 2000). The other reason is the obvious difference between observed and theoretical number density of galaxies at the low velocity region ($v_c < 200\mathrm{km/s}$). The reason of this difference is that in our model we neglect effects of e.g., supernovae feedback (Dekel & Silk 1986) which substantially suppress the number of galaxies in low-mass halos (e.g., Gonzalez et al. 2000; Nagamine et al. 2001). However we are interested in the gravitational lensing with angular separation larger than current angular resolution ($\theta \sim 0.3''$), thus we can safely neglect such low-velocity galaxies which have little impact on our lensing results.

Figure 1 shows constraints on model parameters from observed velocity functions. Contours are calculated from ratios of combined likelihood $\mathcal{L} \propto \prod \exp(-\frac{1}{2}\chi_i^2)$. Errors of observed velocity functions are estimated from errors of fitting parameters of velocity functions (see Gonzalez et al. 2000). As easily seen from the upper panel of Figure 1, we can put useful constraints on δ_h and $v_h \equiv v_c(M_h)$. The best fit parameter set is $(\delta_h, v_h) \simeq (0.78, 238\mathrm{km/s})$. This means that there still remains strong degeneracy between M_h and γ_v: parameter combinations which yield the same v_h cannot be discriminated from the velocity functions. This fact is also shown in the lower panel of Figure 1. One of our best fit parameter

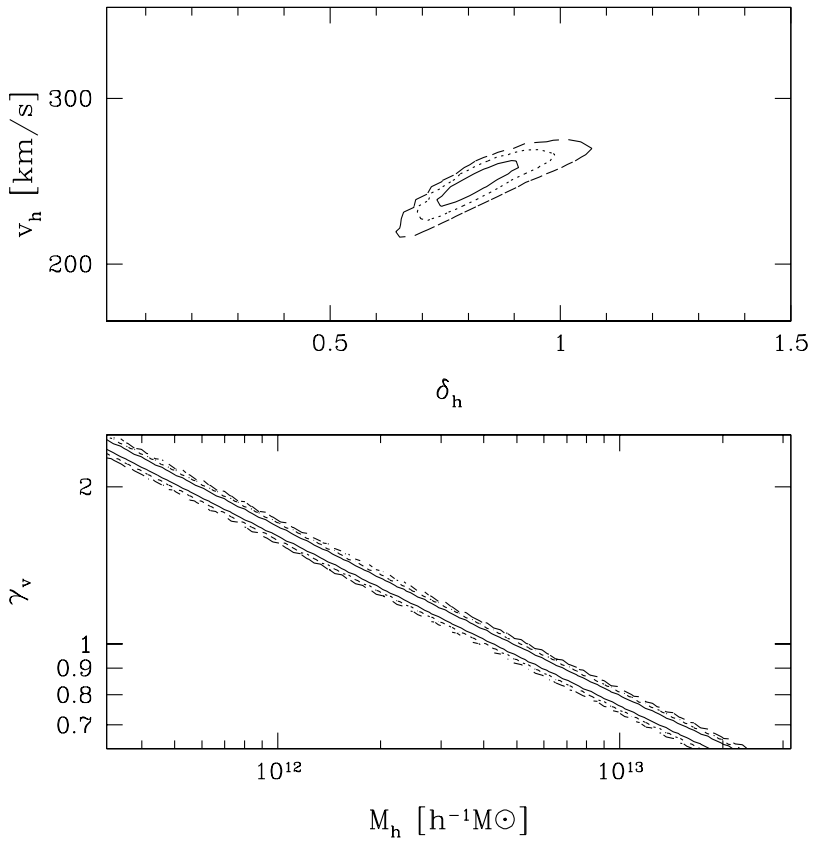

FIG. 1.— Constraints on model parameters from the velocity function of galaxies. 68% (*solid*), 95% (*dotted*), and 99% (*dashed*) likelihood contours are shown. Upper panel: constraint on δ_h and $v_h \equiv v_c(M_h)$. Lower panel: constraint on M_h and γ_v assuming $\delta_h = 0.78$.

sets $(\delta_h, M_h, \gamma_v) = (0.78, 10^{12}h^{-1}M_\odot, 1.67)$ is compared with observed velocity functions in Figure 2. It is clearly shown that the prediction of our model shows good coincidence with observed velocity functions.

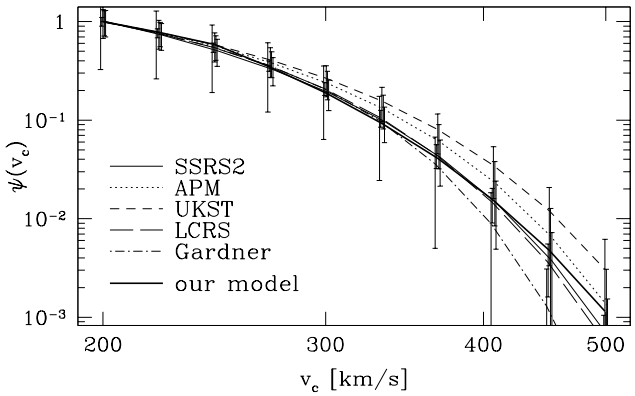

FIG. 2.— One of our best fit models for the velocity function is compared with the five observed velocity functions (Gonzalez et al. 2000). Here normalized velocity functions (eq. [16]) are compared. Errorbars are estimated from the error of fitting parameters of velocity functions. The model parameters are chosen so as to satisfy constrains in Figure 1: $\delta_h = 0.78$, $M_h = 10^{12}h^{-1}M_\odot$, and $\gamma_v = 1.67$.

3.2. *Image Separation Distribution*

The distribution of image separations in strong gravitational lensing becomes another test of our model. The distribution is calculated from equation (15). For the observed lens sample, we consider the Cosmic Lens All-Sky Survey (CLASS; Helbig 2000). This sample is complete at image separations $0.3'' < \theta < 15''$ (Helbig 2000; Phillips et al. 2001), and has 18 lenses among $\sim 12,000$ radio sources. Sources have the flux distribution $dn/dS \propto S^{-2.1}$ (Rusin & Tegmark 2001). The mean redshift is estimated to be $\langle z_S \rangle = 1.27$, although the redshift distribution of sources is still poorly understood (Marlow et al. 2000). As in the case of the velocity function, actually we consider the normalized image separation distribution:

$$p(>\theta; z_S, L) = \frac{P(>\theta; z_S, L)}{P(>0.3''; z_S, L)}, \tag{17}$$

instead of usual probability distribution. This is because the absolute probability may suffer from uncertainties of source redshifts, magnification bias, and cosmological parameters. On the other hand the distribution $p(>\theta)$ mainly contains information on the shape of the mass function and effects of baryonic compression (Kochanek 2001; Kochanek & White 2001; Keeton 2001). And the distribution $p(>\theta)$ is quite insensitive to the source population and cosmological parameters, thus can be used for samples in which the source population is unknown such as CASTLES sample.

The distribution of image separations is tested by using a Kolmogorov-Smirnov (KS) test. For the observed distribution, we use the distribution of CLASS survey. The result is shown in Figure 3. We plot contours in M_h-γ_v plane by fixing $\delta_h = 0.78$ which is constrained from the velocity function (see Figure 1). From this figure, we find that the constraint from the distribution of image separations is consistent with the constraint from the velocity function. The exception is the case of $\alpha = 1.5$, where α is the inner slope of the density profile of dark halos

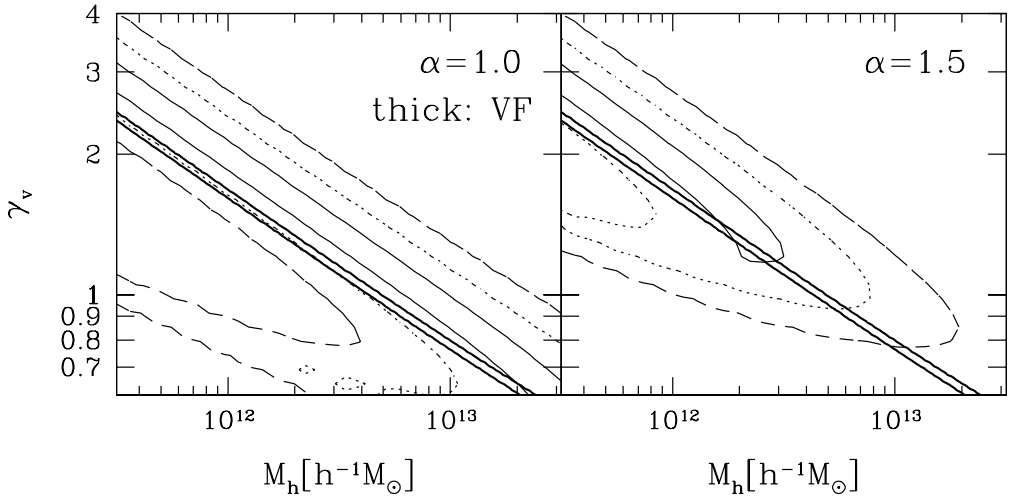

FIG. 3.— Constraints on model parameters from the distribution of image separations in strong gravitational lensing. Here we have assumed $\delta_{\rm h} = 0.78$. 68% (*solid*), 95% (*dotted*), and 99% (*dashed*) contours are calculated using Kolmogorov-Smirnov test. 68% constraint from the velocity function (see Fig. 1) is also plotted by thick lines. For the inner slope of the density profile of dark halos (eq. [2]), we consider both $\alpha = 1.0$ (*left*) and $\alpha = 1.5$ (*right*).

(eq. [2]). In this case, the lower value of γ_ν becomes inconsistent with the observation, because the lensing cross section for SIS is $\sigma_{\rm SIS} \propto \gamma_\nu^4$ (see eq. [11]) and the lower value of γ_ν means that the contribution of dark halo lenses becomes more significant. That is, when γ_ν is low, the number of dark halo lenses is comparable to that of galaxy lenses, thus a steep cutoff in the distribution of image separations never appears. Therefore, we conclude that the constraint from the distribution of image separations is consistent with the constraint from the velocity function, except for the cutoff of KS probability at low γ_ν which may appear when α is large. We also compare the distribution of our model with the observed distribution in Figure 4. The model parameters are chosen so as to satisfy the constraint from the velocity function, and same as those used in Figure 2. We also plot the distribution assuming that all lens objects are well approximated by SIS. This assumption corresponds to $p_{\rm g}(M) = 1$ for all M. It is obvious that our model well reproduces the observed distribution while the distribution of all SIS assumption is far from the observed distribution, as pointed out by Keeton (1998).

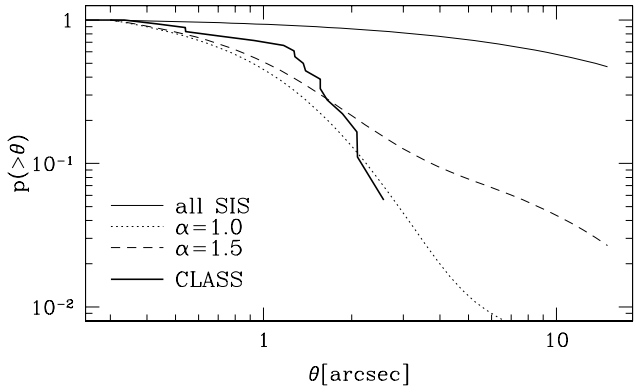

FIG. 4.— The distribution of image separations in gravitational lensing (eq. [17]). The model parameters are same as Figure 2. The cases with $\alpha = 1.0$ (*dotted*) and $\alpha = 1.5$ (*dashed*) are plotted. The observed distribution in CLASS survey is shown by thick solid line. The thin solid line indicates the theoretical distribution assuming all lens objects are SIS lenses. This corresponds to $p_{\rm g}(M) = 1$ for all M.

3.3. *Various Constraints on the Circular Velocity of Galaxies*

In §3.1 and §3.2, we constrained model parameters from the velocity function of galaxies and the distribution of image separations. The strong degeneracy between $M_{\rm h}$ and γ_ν, however, still remains. Therefore in this subsection we try to put constraints on γ_ν from various theories and observations. We consider following three constraints.

First, Seljak (2002a) gave values of γ_ν at several halo mass derived from the observation and analysis of galaxy-galaxy lensing (McKay et al. 2002; Guzik & Seljak 2002) and Tully-Fisher/fundamental plane relations. The observation of galaxy-galaxy lensing allows us to determine the mass of dark halos and its relation to the luminosity of galaxies. Tully-Fisher/fundamental plane relations are used to derive the galaxy circular velocity from its luminosity. He found that γ_ν is significantly larger than 1, $\gamma_\nu \sim 1.8$ around L_*. He also found the decrease of γ_ν from L_* to $7L_*$, $\gamma_\nu \sim 1.4$ at $7L_*$.

Second, Cole et al. (2000) semi-analytically calculated average values of γ_ν for galaxies with $-20 < M_I - 5\log h < -18$. They calculated γ_ν for various parameter sets of semi-analytic model, and found that most of parameter sets predict $\gamma_\nu \sim 1.3$–1.4. The most important parameter for γ_ν is the baryon density $\Omega_{\rm b}$, but even in the extreme cases they examined, $\Omega_{\rm b} = 0.01$ and 0.04, γ_ν becomes 1.13 and 1.96, respectively.

Third, Mo et al. (1998) considered the analytic disk formation model on the basis of adiabatic compression (e.g., Blumenthal et al. 1986). In their model, γ_ν depends on the mass of cooled baryons and the angular momentum of galactic disc. More specifically, their model is characterized by following three parameters; the concentration parameter c, the ratio of disk mass to halo mass $m_{\rm d}$, and the angular momentum λ' (see Mo et al. 1998). We assume that the concentration parameter is related to halo mass as in equation (3). Then γ_ν at fixed mass depends on $m_{\rm d}$ and λ'. We examine following two extreme cases: $(m_{\rm d}, \lambda') = (0.02, 0.02)$ and $(0.02, 0.2)$. Most of parameter sets which are physically reasonable predict the value of γ_ν between these two extreme cases.

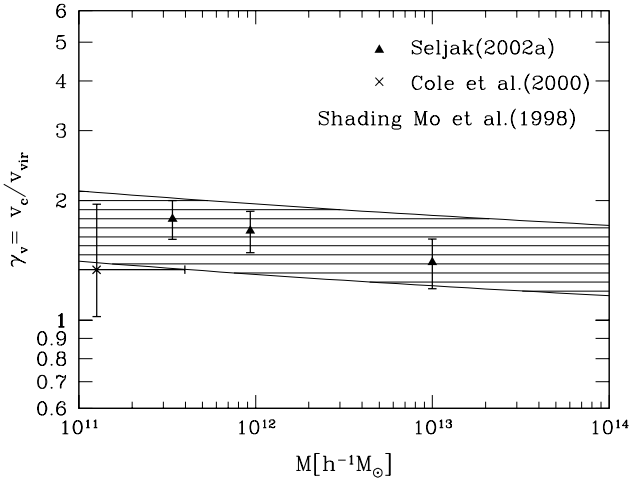

FIG. 5.— Constraints on γ_v from various models. (i) Seljak (2002a) gave values of γ_v at several halo mass derived from the observation and analysis of galaxy-galaxy lensing (McKay et al. 2002; Guzik & Seljak 2002) and Tully-Fisher/fundamental plane relations. Errorbars indicate 1σ level error. (ii) Cole et al. (2000) semi-analytically calculated the average values of γ_v for various parameter sets of semi-analytic model. The errorbar in the direction of γ_v-axis means that all parameter sets predict γ_v within this range. (iii) In the analytic disk formation model of Mo et al. (1998), γ_v depends on the mass of cooled baryons and the angular momentum of galactic disc. Any choice of these two parameters which is physically allowed, however, results in the value of γ_v in the shading region.

The result is summarized in Figure 5. Particularly we are interested in the strong gravitational lensing, thus we focus on the range $10^{12}h^{-1}M_\odot \lesssim M \lesssim 10^{13}h^{-1}M_\odot$ where gravitational lensing with separations $\theta > 0.3''$ is most efficient. In this range of halo mass, various constraints indicate that γ_v is restricted to $1 \lesssim \gamma_v \lesssim 2$. In particular, the upper bound of γ_v is quite robust because γ_v is closely related to the amount of cooled baryons; to produce $\gamma_v \gg 2$, we need the extraordinarily large amount of cooled baryon which exceeds the global baryon mass ratio (Seljak 2002a). Figure 5 also indicates that γ_v should slightly depend on halo mass. The mass dependence of γ_v, however, is not so important because our interest is restricted in a narrow mass range. Therefore we can safely assume that γ_v is constant.

4. THE FRACTION OF DARK HALO LENSES

According to the model described in §2, we predict the fraction of dark halo lenses. In our model, there are three parameters which govern effects of baryonic compression; δ_h, M_h, and γ_v. Since the constraint from the velocity function of galaxies (§3.1) indicates that δ_h should be restricted around $\delta_h \sim 0.78$, we fix $\delta_h = 0.78$ in the remainder of this paper. On the other hand, the other parameters, M_h and γ_v, were poorly constrained from the velocity function of galaxies and the distribution of image separations. Therefore we should see the dependence of the fraction of dark halo lenses on both M_h and γ_v. Another important parameter we should examine is the inner slope of density profile (α in eq. [2]), because it is also known that the number of dark halo lenses is extremely sensitive to α (Wyithe et al. 2001; Keeton & Madau 2001; Takahashi & Chiba 2001; Li & Ostriker 2002; Oguri et al. 2002).

The fraction of dark halo lenses at image separations $\theta_1 < \theta < \theta_2$ is given by

$$f_{\rm dark}(\theta_1 < \theta < \theta_2) = \frac{P_{\rm dark}(>\theta_1) - P_{\rm dark}(>\theta_2)}{P(>\theta_1) - P(>\theta_2)}, \qquad (18)$$

where $P_{\rm dark}(>\theta)$ and $P(>\theta)$ are calculated from equations (10) and (15), respectively. Again, $f_{\rm dark}$ is almost independent of the source population (source redshift and flux distribution) and cosmological parameters because these primarily change the normalization of the overall lensing rate which we never use. For the range of image separations, we consider following two cases: (1) $0.3'' < \theta < 15''$. In this range of image separations, CLASS survey is complete (Helbig 2000; Phillips et al. 2001). Among 18 lenses observed in CLASS survey, virtually all lenses are known to be galaxy lenses (Rusin 2002). (2) $0.3'' < \theta < 3''$. Most of current ambiguous quasar pairs which may be dark halo lenses have separations $\theta > 3''$ and almost all lenses with smaller separations are known to be produced by normal galaxies (Kochanek et al. 1999; Rusin 2002). Therefore, in this case we can use all lenses with separations $0.3'' < \theta < 3''$ in comparison with our result. Below we assume that there is no dark halo lens for both cases.

Figure 6 plots contours of $f_{\rm dark}$ in M_h-γ_v plane. The constraint from the velocity function of galaxies is also shown. From this figure, it is found that the fraction of dark halo lenses is sensitive to γ_v: $f_{\rm dark}$ increases as γ_v decreases. The reason is that the cross section of SIS lenses scales as $\sigma_{\rm SIS} \propto \gamma_v^4$ (see eq. [11]) and the number of galaxy lenses decreases as γ_v decreases. The fraction of dark halo lenses also increases as M_h decreases, because the number of dark halos which act as dark halo lenses becomes large. Figure 6 indicates that $f_{\rm dark}$ cannot be determined uniquely, even if we restrict M_h and γ_v such that they satisfy the constraint from the velocity function of galaxies. This fact is clearly shown in Figure 7. In Figure 7, we plot $f_{\rm dark}$ as a function of γ_v. The parameter M_h is chosen so that it satisfies the constraint from the velocity function of galaxies. This figure indicates that $f_{\rm dark}$ is sensitive to γ_v. Even if we restrict $1 \le \gamma_v \le 2$ as discussed in §3.3, $f_{\rm dark}$ has uncertainty of about one order of magnitude. Figure 7 also shows that $f_{\rm dark}$ is sensitive to α. From $\alpha = 1.0$ to 1.5, $f_{\rm dark}$ also changes about one order of magnitude. Therefore, our conclusion is that robust predictions of $f_{\rm dark}$ need information on both γ_v and α. If the density profile of dark halos is determined from several observations, we can break the degeneracy between M_h and γ_v from the observation of $f_{\rm dark}$.

Although $f_{\rm dark}$ strongly depends on γ_v, we obtain the lower limit $f_{\rm dark,min}$ by restricting γ_v. Discussions in §3.3 suggest that it is safe to adopt $\gamma_v \le 2$. Thus by setting $\gamma_v = 2$ we can derive $f_{\rm dark,min}$, which is shown in Figure 8. In this figure $f_{\rm dark,min}$ is plotted against the inner slope α. The lack of dark halo lenses places upper limit on the value of $f_{\rm dark}$ which is also shown in Figure 8. From this figure, we find that too cuspy inner slope of dark halos ($\alpha \gtrsim 1.5$) is inconsistent with the lack of dark halo lenses: even if we adopt sufficiently large γ_v, $\gamma_v = 2$, we predict too much dark halo lenses to reconcile with the observation. This constraint has somewhat different meaning from the one derived from the statistics of wide separation lensing (Keeton & Madau 2001; Li & Ostriker 2002) because such statistics may suffer from the uncertainties of cosmological parameters and the source population.

Are there any other effects which may change $f_{\rm dark}$? We consider following two effects which may change our results. One is the effect of "substructures" (i.e., galaxies in groups and clusters) as discussed in §2.2. Substructures may affect the fraction of dark halo lenses directly, because it changes only the number of galaxy lenses. Moreover the situation that lens galaxies which lie in groups or clusters is not rare (e.g., Q0957+561), thus the effect should be addressed quantitatively. Although the effect of substructures seems difficult to estimate, Keeon,

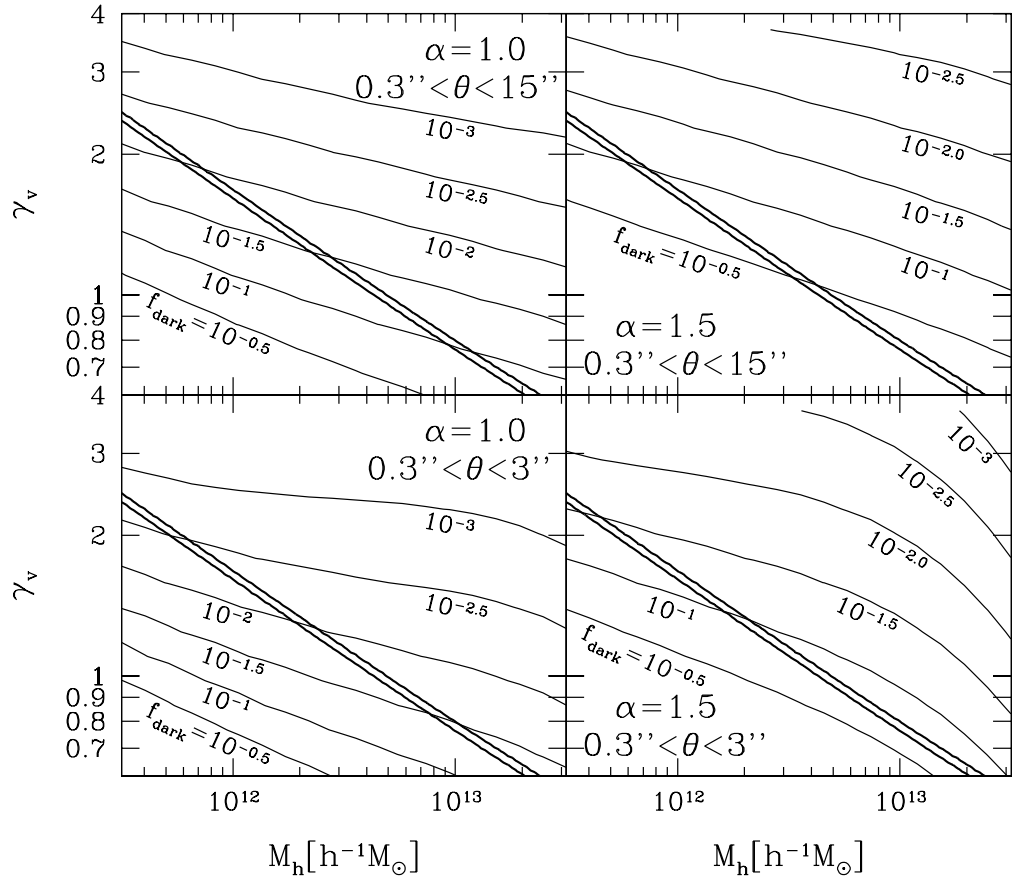

FIG. 6.— Contour plots for the fraction of dark halo lenses in $M_{\rm h}$-$\gamma_{\rm v}$ plane. Thick lines are 68% contours derived from the velocity function (see Fig. 1). The inner cusps of dark halos (eq. [2]) are $\alpha = 1.0$ (*left*) and $\alpha = 1.5$ (*right*). For the range of image separations, $0.3'' < \theta < 15''$ (*upper*) and $0.3'' < \theta < 3''$ (*lower*) are considered.

Christlein, & Zabludoff (2000) calculated the fraction of lensing galaxies which lie in groups and clusters. They predicted that $\sim 25\%$ of lens galaxies are likely to be in groups or clusters. Following this, the effect of substructures are simply estimated by replace the probability of galaxy lensing as $P_{\rm gal} \to (4/3)P_{\rm gal}$. This decreases $f_{\rm dark}$ by a factor $3/4$ at most. The fraction of dark halo lenses including this effect is also displayed in Figure 8. As seen in the figure, our result that $\alpha \gtrsim 1.5$ is inconsistent with the observation is not so affected by the effect of substructures. The other effect is the existence of "empty halos", that is, dark halos which do not host a galaxy. We have adopted the galaxy formation probability $p_{\rm g}(M)$ of the form (1), and this means that we have assumed there is no empty halo at $M < M_{\rm h}$. Although this assumption does not conflict with the observation of galaxy-galaxy lensing (Seljak 2002b), it is still possible that the significant amount of empty halos exists at galaxy-mass scale. This effect, however, only *increases* $f_{\rm dark}$. Therefore *lower limit* of $f_{\rm dark}$ used in Figure 8 is never changed by this effect.

The main result of Wyithe et al. (2001) and Keeton & Madau (2001) is that the lensing probability of dark halos depends strongly on the choice of concentration parameters as well as inner slopes α. Therefore, in Figure 9 we examine $f_{\rm dark,min}$ for different concentration parameters. In calculating this, we adopt the concentration parameter of the following form:

$$c_{\rm vir}(M,z) = \frac{c_{\rm norm}}{1+z}\left(\frac{M}{10^{14}h^{-1}M_\odot}\right)^{-0.13}, \qquad (19)$$

instead of equation (3), and regard $c_{\rm norm}$ as a free parameter. We plot $f_{\rm dark,min}$ in α-$c_{\rm norm}$ plane. From this figure, it is clearly seen that there is a strong degeneracy between α and $c_{\rm norm}$ as reported by Wyithe et al. (2001) and Keeton & Madau (2001). Thus actually we can constrain the combination of α and $c_{\rm norm}$, or the core mass fraction proposed by Keeton & Madau (2001), instead of α and $c_{\rm norm}$ separately.

5. CONCLUSION

We have studied the effect of baryonic compression assuming the simple parametric model used by Kochanek (2001). Our model has following two elements: the galaxy formation probability $p_{\rm g}(M)$ (eq. [1]) which describes the global efficiency of baryonic compression, and the ratio of circular velocities of galaxies to virial velocities of dark halos $\gamma_{\rm v} = v_{\rm c}/v_{\rm vir}$ which means how the inner structure of dark halos is modified due to baryonic compression. The model parameters are constrained from the observed velocity function of galaxies and the distribution of image separations in strong gravitational lensing, although the strong degeneracy between model parameters still remains. By using this model, we predict the fraction of dark halo lenses $f_{\rm dark}$ (eq. [18]). Here dark halo lenses mean the lens systems which are produce by the gravitational potential of dark halos. The fraction of dark halo lenses is independent of the normalization of total lensing rate, thus is insensitive to cosmological parameters and information of sources such as redshift and flux distribution. Instead the fraction of dark halo lenses is expected to have information on both the effect of baryonic compression and the density profile of dark halos such as the

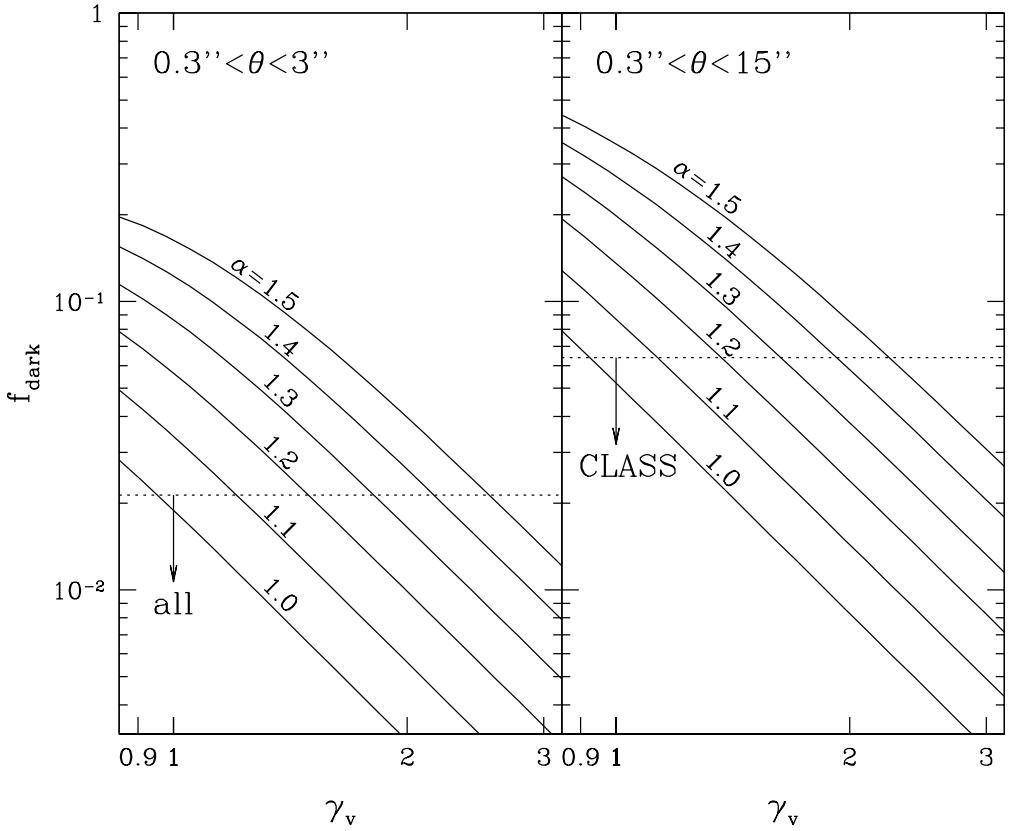

FIG. 7.— The fraction of dark halo lenses as a function of γ_v. Each solid line is the result with particular choice of α. For each γ_v, the value of M_h is chosen so that it satisfies the constraint from the velocity function. Observational upper limits of f_{dark} at 1σ level (all lenses and the CLASS survey lenses) are also shown by dotted lines with downward arrows.

inner density profile for which we modeled $\rho \propto r^{-\alpha}$. We found that f_{dark} is indeed sensitive to the inner slope α, concentration parameter c_{norm}, and model parameters such as γ_v. Therefore, definite predictions of f_{dark} need correct knowledge of baryonic compression as well as the density profile of dark halos. This also means that we can constrain the model of baryonic compression from the observation of f_{dark} if the density profile of dark halos is well known.

Although the fraction of dark halo lenses is difficult to predict, we can still derive the lower limit of f_{dark} by restricting $\gamma_v \leq 2$ which is inferred from various theories and observations (see §3.3). We found that the steep inner profiles ($\alpha \gtrsim 1.5$) or too centrally concentrated dark halos are inconsistent with the lack of dark halo lenses in observations. As described above, our result is quite insensitive to cosmological parameters and source population. Therefore, our result is complementary to the result of Keeton & Madau (2001) who obtained similar constraint on the density profile of dark halos using the total lensing probability which also depends strongly on cosmological parameters. One of possible systematic effects which may change f_{dark} is the effect of galaxies in groups or clusters. By using the result of Keeton et al. (2000), we found that this effect changes f_{dark} by a factor $3/4$ at most. Therefore this effect does not change our main result so much. Other important systematic effect is the existence of empty halos which are neglected in our model. This effect is, however, not important for the lower limit of f_{dark}, because this effect only increases the fraction of dark halo lenses.

One possible criticism of our result is that the baryon compression model we use in this paper is too simple. Many of the previous work, however, have not addressed this problem. For example, most work of gravitational lensing statistics which use the mass function of dark halos assumed that circular velocities of galaxies are the same as virial velocities of dark halos (this corresponds to $\gamma_v = 1$ in our model). But this assumption seems to be invalid (e.g., Seljak 2002a), and since the number of galaxy lenses scales as $\propto \gamma_v^4$ the deviation from $\gamma_v = 1$ should not be dismissed. This fact is seen even in our simple model where the connection between galaxy lenses and dark halo lenses sensitively depends on γ_v, and is indeed difficult to be determined. The importance of baryonic compression, however, means that we can constrain the model of baryonic compression from observations of the fraction of dark halo lenses. Although the current sample of gravitational lensing may be too small for this purpose, the larger lens sample obtained by e.g., SDSS can strongly constrain the model of baryonic compression as well as the density profile of dark halos.

The author would like to thank Yasushi Suto, Atsushi Taruya, and Mamoru Shimizu for useful discussions and comments.

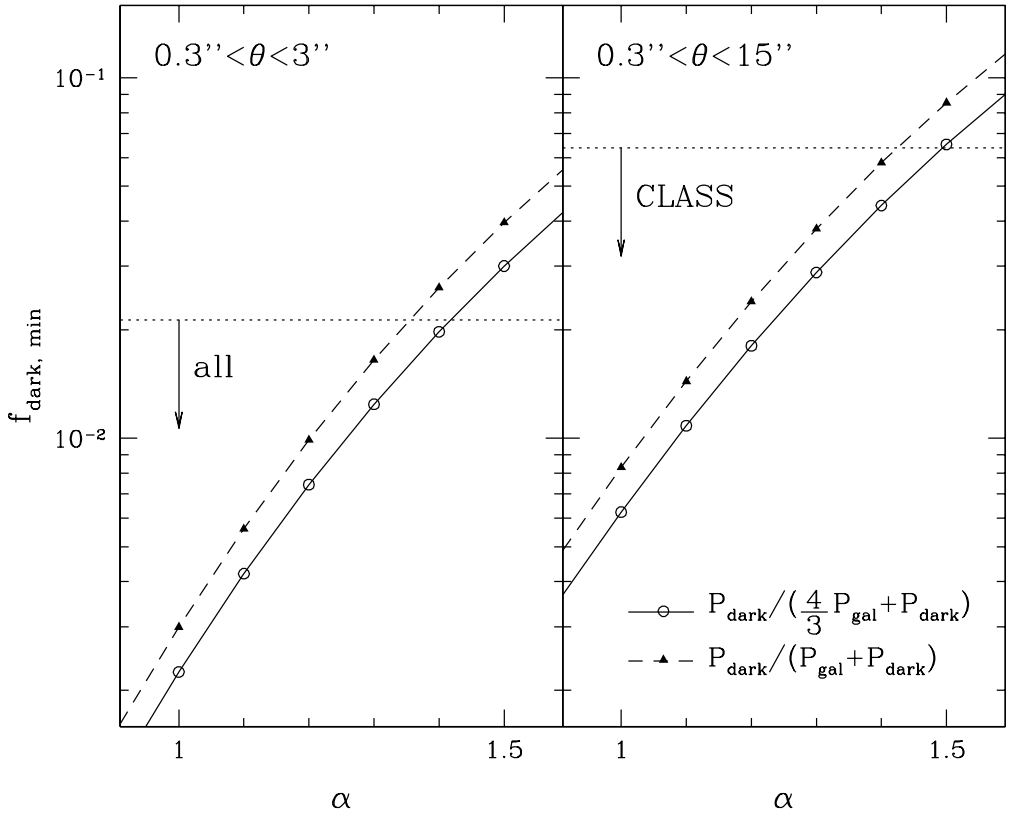

FIG. 8.— The lower limit of $f_{\rm dark}$ as a function of inner slope α, when $\gamma_{\rm v}$ is restricted to $\gamma_{\rm v} \leq 2$. Dashed lines are calculated simply by setting $\gamma_{\rm v} = 2$ in Figure 7. For solid lines, the effect of galaxies which lie in groups/clusters is taken into account (see text for detail). Dotted lines with downward arrows indicate the 1σ constraint from the lack of dark halo lenses in observations.

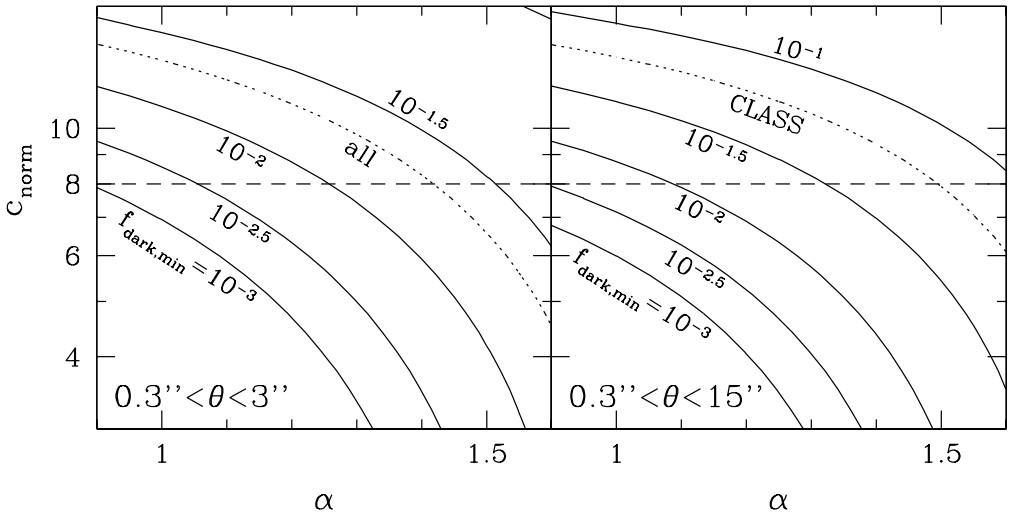

FIG. 9.— Contour plots for the lower limit of $f_{\rm dark}$ in the α-$c_{\rm norm}$ plane. The effect of galaxies in groups/clusters is taken into account. Dotted lines show the 1σ constraint from the lack of dark halo lenses in observations. Dashed lines indicate the value of $c_{\rm norm}$ we used in the previous plots.

REFERENCES

Bartelmann, M., Huss, A., Colberg, J. M., Jenkins, A., & Pearce, F. R. 1998, A&A, 330, 1
Blumenthal, G. R., Faber, S. M., Flores, R., & Primack, J. R. 1986, ApJ, 301, 27
Bullock, J. S., Kolatt, T. S., Sigad, Y., Somerville, R. S., Kravtsov, A. V., Klypin, A. A., Primack, J. R., & Dekel, A. 2001, MNRAS, 321, 559
Cen, R., Gott, J. R., Ostriker, J. P., & Turner, E. L. 1994, ApJ, 423, 1
Chiba, M., & Yoshii, Y. 1999, ApJ, 510, 42
Cohn, J. D., Kochanek, C. S., McLeod, B. A., & Keeton, C. R. 2001, ApJ, 554, 1216
Cole, S., & Kaiser, N. 1989, MNRAS, 237, 1127
Cole, S., Lacey, C. G., Baugh, C. M., & Frenk, C. S. 2000, MNRAS, 319, 168
Dekel, A., & Silk, J. 1986, ApJ, 303, 39
Fukugita, M., Futamase, T., Kasai, M., & Turner, E. L. 1992, ApJ, 393, 3
Fukugita, M., & Turner, E. L. 1991, MNRAS, 253, 99
Fukushige, T., & Makino, J. 2001, ApJ, 557, 533
Fukushige, T., & Makino, J. 2002, ApJ, submitted (astro-ph/0108014)
Gardner, J. P., Sharples, R. M., Frenk, C. S., & Carrasco, B. E. 1997, ApJ, 480, L99
Ghigna, S., Moore, B., Governato, F., Lake, G., Quinn, T., & Stadel, J. 2000, ApJ, 544, 616

Gonzalez, A. H., Williams, K. A., Bullock, J. S., Kolatt, T. S., & Primack, J. R. 2000, ApJ, 528, 145
Guzik, J., & Seljak, U. 2002, MNRAS, in press (astro-ph/0201448)
Helbig, P. 2000, preprint (astro-ph/0008197)
Jing, Y. P. 2000, ApJ, 535, 30
Jing, Y. P., & Suto, Y. 2000, ApJ, 529, L69
Keeton, C. R. 1998, Ph. D. thesis, Harvard Univ.
Keeton, C. R. 2001, ApJ, 561, 46
Keeton, C. R., Christlein, D., & Zabludoff, A. I. 2000, ApJ, 545, 129
Keeton, C. R., & Madau, P. 2001, ApJ, 549, L25
Kitayama, T., & Suto, Y. 1996, ApJ, 469, 480
Klypin, A., Kravtsov, A. V., Bullock, J. S., & Primack, J. R. 2001, ApJ, 554, 903
Kochanek, C. S. 1995, ApJ, 453, 545
Kochanek, C. S. 1996, ApJ, 466, 638
Kochanek, C. S. 2001, in STScI spring symposium, The Dark Universe: Matter, Energy, and Gravity, ed. M. Livio (Cambridge University Press), in press (astro-ph/0108160)
Kochanek, C. S., Falco, E. E., & Muñoz, J. A. 1999, ApJ, 510, 590
Kochanek, C. S., & White, M. 2001, ApJ, 559, 531
Lacey, C., & Cole, S. 1993, MNRAS, 262, 627
Li, L. X., & Ostriker, J. P. 2002, ApJ, 566, 652
Maoz, D., & Rix, H.-W. 1993, ApJ, 416, 425
Maoz, D., Rix, H.-W., Gal-Yam, A., & Gould, A. 1997, ApJ, 486, 75
Marlow, D. R., Rusin, D., Jackson, N., Wilkinson, P. N., Browne, I. W. A., & Koopmans, L. 2000, AJ, 119, 2629
McKay T. A., et al. 2002, ApJ, submitted (astro-ph/0108013)
Meneghetti, M., Yoshida, N., Bartelmann, M., Moscardini, L., Springel, V., Tormen, G., & White S. D. M. 2001, MNRAS, 325, 435
Mo, H. J., Mao, S., & White, S. D. M. 1998, MNRAS, 295, 319
Molikawa, K., & Hattori, M. 2001, ApJ, 559, 544
Moore, B., Quinn, T., Governato, F., Stadel, J., & Lake, G. 1999, MNRAS, 310, 1147
Mortlock, D. J., & Webster, R. L. 2000, MNRAS, 319, 872
Nagamine, K., Fukugita, M., Cen, R., & Ostriker, J. P. 2001, MNRAS, 327, L10
Nakamura, T. T., & Suto, Y. 1997, Prog. Theor. Phys., 97, 49
Narayan, R., & White, S. D. M. 1988, MNRAS, 231, 97P
Navarro, J. F., Frenk, C. S., & White, S. D. M. 1996, ApJ, 462, 563
Navarro, J. F., Frenk, C. S., & White, S. D. M. 1997, ApJ, 490, 493
Oguri, M. 2002, ApJ, 573, 51
Oguri, M., Taruya, A., & Suto, Y. 2001, ApJ, 559, 572
Oguri, M., Taruya, A., Suto, Y., & Turner, E. L. 2002, ApJ, 568, 488
Phillips, P. M., et al. 2001, MNRAS, 328, 1001
Porciani, C., & Madau, P. 2000, ApJ, 532, 679
Power, C., Navarro, J. F., Jenkins, A., Frenk, C. S., White, S. D. M., Springel, V., Stadel, J., & Quinn, T. 2002, MNRAS, submitted (astro-ph/0201544)
Press, W. H., & Schechter, P. 1974, ApJ, 187, 425
Rix, H.-W., de Zeeuw, P. T., Cretton, N., van der Marel, R. P., & Carollo, C. M. 1997, ApJ, 488, 702
Rusin, D. 2002, ApJ, 572, 705
Rusin, D., & Ma, C.-P. 2001, ApJ, 549, L33
Rusin, D., & Tegmark, M. 2001, ApJ, 553, 709
Sarbu, N., Rusin, D., & Ma, C.-P. 2001, ApJ, 561, L147
Schneider, P., Ehlers, J., & Falco, E. E. 1992, Gravitational Lenses (New York: Springer)
Seljak, U. 2002a, MNRAS, in press (astro-ph/0201450)
Seljak, U. 2002b, MNRAS, submitted (astro-ph/0203117)
Sheth, R. K., & Tormen, G. 1999, MNRAS, 308, 119
Shimasaku, K. 1993, ApJ, 413, 59
Takahashi, R., & Chiba, T. 2001, ApJ, 563, 489
Turner, E. L. 1980, ApJ, 242, L135
Turner, E. L. 1990, ApJ, 365, L43
Turner, E. L., Ostriker, J. P., & Gott, J. R. 1984, ApJ, 284, 1
Walsh, D., Carswell, R. F., & Weymann, R. J. 1979, Nature, 279, 381
Wambsganss, J., Cen, R., & Ostriker, J. P. 1998, ApJ, 494, 29
Wambsganss, J., Cen, R., Ostriker, J. P., & Turner, E. L. 1995, Science, 268, 274
Williams, L. L. R., Navarro, J. F., & Bartelmann, M. 1999, ApJ, 527, 535
Wyithe, J. S. B., Turner, E. L., & Spergel, D. N. 2001, ApJ, 555, 504
Yoshikawa, K., Taruya, A., Jing, Y. P., & Suto, Y. 2001, ApJ, 558, 520
Zhao, H. S. 1996, MNRAS, 278, 488